Synthesis, crystal structure and optical properties of $Na_2RE(PO_4)(WO_4)$ (RE = Y, Tb–Lu)†

Michael Daub,[a,b] Anna J. Lehner[b] and Henning A. Höppe*[a]

Phase-pure samples of sodium rare-earth phosphate tungstates $Na_2RE(PO_4)(WO_4)$ (RE = Y, Dy–Lu) and $Na_2Y(PO_4)(WO_4):Ln^{3+}$ (Ln = Eu, Tb) were obtained by reaction of the respective rare-earth oxide with ammonium hydrogen phosphate with sodium tungstate $Na_2WO_4 \cdot 2H_2O$ as a flux at 1220 K. According to X-ray single-crystal investigations $Na_2RE(PO_4)(WO_4)$ (RE = Y, Tb–Lu) crystallise orthorhombically in space group *Ibca* (no. 73) (RE = Y, Z = 8, a = 1799.7(4), b = 1210.2(2), c = 683.82(14) pm, wR_2 = 0.040, R_1 = 0.037, 661 reflections, 62 parameters). The crystal structure contains non-condensed phosphate and tungstate tetrahedra with the (3 + 3)-coordinate sodium and eight-coordinate rare-earth ions in the voids. Relevant absorption and infrared spectra as well as the fluorescence spectra of $Na_2Y(PO_4)(WO_4):Ln^{3+}$ (Ln = Eu, Tb) are presented. An FP-LAPW band-structure calculation confirms the assignment of the main absorption as well as the optical band-gap (ε_{calc} = 5.1 eV; ε_{meas} = 5.2(1) eV) of $Na_2Y(PO_4)(WO_4)$.

1 Introduction

Sensitised luminescence is a very important opportunity to improve the luminescence properties of emitters with parity forbidden transitions or their sensitisation for desired wavelengths. The respective activator can be sensitised for certain wavelength absorptions by using an efficient sensitiser's absorption and subsequent energy transfer onto the activator. Moreover, the overall luminescence efficiency may be improved by using sensitisers with broad absorption bands. In complex chemistry this is known as the antenna effect.[1] A similar approach for ionic solids was presented by Blasse approximately fifty years ago; he showed that activators like Eu^{3+} or Tb^{3+} may be sensitised by doping these into tungstates like $Y_2(WO_6)$.[2] Tungstates are possible sensitisers since transition metal compounds in highest oxidation states provide efficient charge-transfer transitions. This energy may then be emitted directly thereafter or transferred onto other emitters present in the phosphor.

While in $Y_2(WO_6)$ any octahedral tungstate antenna serves formally two rare-earth ions we decided to investigate the rare-earth phosphate tungstates $Na_2RE(PO_4)(WO_4)$ (RE = Y, Tb–Lu) in which any tungstate antenna serves only a single rare-earth ion. A second positive effect compared to stoichiometric tungstates might be a reduced concentration quenching since the average distance between the luminescent centres is larger. So far chemically similar compounds like $Na_2Y(PO_4)(MoO_4)$,[3,4]

$Na_2RE(PO_4)(MoO_4)$ (RE = Tb–Lu),[5] $A_2Yb(PO_4)(MoO_4)$ (A = Na, K),[6] $K_2Eu(PO_4)(MoO_4)$,[7] $K_2M(PO_4)(MoO_4)$ (M = Bi, Ho),[8,9] $K_2Bi(PO_4)(MoO_4)$,[10] $Cs_2Bi(PO_4)(MoO_4)$[11] and $K_2Sm(PO_4)(MoO_4)$[12] have been structurally characterised. First optical investigations on species doped with trivalent europium were recently presented for $Na_2Bi(PO_4)(MO_4):Eu^{3+}$ (M = Mo, W).[13]

In our contribution we present detailed crystal structure investigations on the phosphate tungstates $Na_2RE(PO_4)(WO_4)$ (RE = Y, Tb–Lu) as well as the results of first doping experiments on $Na_2Y(PO_4)(WO_4)$ doped with trivalent europium and terbium, respectively.

2 Experimental section

2.1 Synthesis

The synthesis of the pure as well as the doped $Na_2RE(PO_4)$-(WO_4) (RE = Y, Tb–Lu) was performed according to eqn (1), starting from stoichiometric amounts of ammonium hydrogen phosphate and rare-earth oxide with an excess of sodium tungstate.

$$RE_2O_3 + 2Na_2WO_4 \cdot 2H_2O + 2(NH_4)_2HPO_4$$
$$\rightarrow 2Na_2RE(PO_4)(WO_4) + 4NH_3 + 7H_2O \quad (1)$$
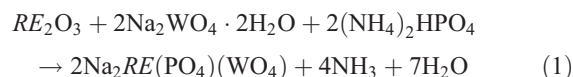
Typical synthesis procedures for the doped phases follow that of $Na_2Y_{0.86}Eu_{0.14}(PO_4)(WO_4)$. A mixture of 97.7 mg (0.433 mmol) yttrium oxide Y_2O_3 (Kristallhandel Kelpin, 99.99%), 26.1 mg (0.074 mmol) europium oxide Eu_2O_3 (Chempur, 99.99%), 145.0 mg (1.098 mmol) diammonium hydrogen phosphate $(NH_4)_2HPO_4$ (ABCR, 98%) and 1.6 g (4.9 mmol) sodium tungstate hydrate $Na_2WO_4 \cdot 2H_2O$ (Merck, 99.00%) acting also as a flux was transferred into a platinum

[a]Institut für Physik, Universität Augsburg, Universitätsstraße 1, D-86159 Augsburg, Germany. E-mail: henning@ak-hoeppe.de; Fax: +49-(0) 821-598-5955
[b]Institut für Anorganische und Analytische Chemie, Albert-Ludwigs-Universität, Albertstr. 21, D-79104 Freiburg, Germany
†Electronic supplementary information (ESI) available. See DOI: 10.1039/c2dt31358h

crucible. The latter was then heated to 1220 K with a rate of 60 K h^{-1}. After 2 h the mixture was cooled to 1010 K with a rate of 15 K h^{-1} before it was allowed cooling to room temperature with a rate of 180 K h^{-1}. The excess of sodium tungstate was dissolved with hot water. Na$_2$Y(PO$_4$)(WO$_4$):Eu was obtained quantitatively as a crystalline, colourless and non-hygroscopic powder.

2.2 Vibrational spectroscopy

An FTIR spectrum was obtained at room temperature by using a Bruker IFS 66v/S spectrometer. The samples were thoroughly mixed with dried KBr (approx. 2 mg sample, 300 mg KBr) and pressed to pellets. Fig. S1 (ESI†) shows the IR spectrum of Na$_2$Y(PO$_4$)(WO$_4$) in good agreement with the isotypic compound K$_2$Bi(PO$_4$)(MoO$_4$).[10]

2.3 UV-Vis spectroscopy

Optical reflection spectra of Na$_2$RE(PO$_4$)(WO$_4$) (RE = Y, Y$_{0.86}$Eu$_{0.14}$, Tb–Lu) were recorded in reflection geometry using an UV-Vis spectrophotometer (Cary 300 Scan, Agilent) fitted with an integrating sphere. The spectra were recorded from 200 to 800 nm, typically with an acquisition rate of 100 nm min^{-1}.

2.4 Fluorescence spectroscopy

Fluorescence emission and excitation spectra were recorded on a Perkin-Elmer LS55 spectrometer scanning a range from 200 to 700 nm. The obtained data have been corrected for emission and excitation with respect to the Xe plasma excitation source.

3 Crystal structure and crystallographic classification

3.1 Crystal structure determination

Suitable single-crystals of Na$_2$RE(PO$_4$)(WO$_4$) (RE = Y, Tb–Lu) were enclosed in glass capillaries. X-ray diffraction data were collected on a Stoe IPDS II area detection diffractometer and corrected numerically for absorption.[14] The diffraction pattern was indexed on the basis of a body centred orthorhombic unit cell. The crystal structures of Na$_2$RE(PO$_4$)(WO$_4$) (RE = Y, Tb–Lu) were solved by direct methods using SHELXTL[15] in space group Ibca (no. 73) and refined with anisotropic displacement parameters for all atoms.

The relevant crystallographic data and further details of the X-ray data collection are summarised in Table 1. Table 2 shows positional and displacement parameters for all atoms in Na$_2$Y-(PO$_4$)(WO$_4$). In Table 3 selected interatomic distances and angles are listed.

Powder samples of Na$_2$RE(PO$_4$)(WO$_4$) (RE = Y, Tb–Lu) were enclosed in glass capillaries with 0.2 mm diameter and investigated at room temperature in Debye–Scherrer geometry on a STOE Stadi P powder diffractometer with Ge(111)-monochromatised Mo-K$_\alpha$ radiation (linear PSD detector, step width 0.5°, acquisition time: 200 s per step). The powder diffraction patterns are presented in Fig. 1 and S2 (ESI†).

Further details of the crystal structure investigations presented in this work may be obtained from the Fachinformationszentrum Karlsruhe, D-76344 Eggenstein-Leopoldshafen, Germany (crysdata@fiz-karlsruhe.de) on quoting the depository numbers CSD-424742 (Na$_2$Y(PO$_4$)(WO$_4$)), CSD-424739 (Na$_2$Tb(PO$_4$)(WO$_4$)), CSD-424735 (Na$_2$Dy(PO$_4$)(WO$_4$)), CSD-424738 (Na$_2$Ho(PO$_4$)-(WO$_4$)), CSD-424736 (Na$_2$Er(PO$_4$)(WO$_4$)) and CSD-424740 (Na$_2$Tm(PO$_4$)(WO$_4$)), CSD-424741 (Na$_2$Yb(PO$_4$)(WO$_4$)), CSD-424737 (Na$_2$Lu(PO$_4$)(WO$_4$)), CSD-424743 (Na$_2$(Y$_{0.861(5)}$Eu$_{0.139(5)}$)-(PO$_4$)(WO$_4$)), the names of the authors, and citation of this publication.

3.2 Crystal structure

The crystal structures of Na$_2$RE(PO$_4$)(WO$_4$) (RE = Y, Tb–Lu) are isotypic with that of Na$_2$Y(PO$_4$)(MoO$_4$).[3,4] The following crystal structure description uses the example of the yttrium compound. Na$_2$Y(PO$_4$)(WO$_4$) comprises non-condensed phosphate and tungstate tetrahedra. These are arranged in layers perpendicular to [100] with every phosphate layer being followed by two tungstate layers. In this packing the yttrium and sodium ions are arranged in ordered zigzag chains (Fig. 2) and coordinated eight- (yttrium) and six-fold (sodium) by oxygen (Fig. 3 and 4).

The Y–O distances lie between 225.9(4) and 242.1(4) pm. These distances agree well with the sum of the ionic radii of 239 pm (Y–O).[16] The sodium cations are irregularly coordinated six-fold by oxygen and show comparably large thermal displacement parameters (Fig. 4). Apparently the void is too large for the sodium ions. Similar potassium or caesium compounds provide an 8-fold coordination also for the alkaline cations.[10,11] The Na–O distances range from 228.5(7) to 293.2(6) pm with two distinct ranges thus leading to an effective 3 + 3 coordination, which supports the previous argument regarding the relatively large void. These distances agree well with the sum of the ionic radii of 240 pm.[16]

Yttrium zigzag chains are linked by phosphate tetrahedra building a layer parallel to the bc-plane. These layers are similar to those found in the structure of xenotime (REPO$_4$, RE = Y, Gd–Lu).[17] According to Fig. 5, a is not related to the decreasing ionic radii of the rare-earth ions. Contrarily, the remaining two axes lengths show the expected relationship. The latter two run parallel to the xenotime-type layers [REPO$_4$] while a is arranged perpendicularly to these layers. The phosphate tetrahedra of the xenotime-type layers act as spacers eliminating the impact of the rare-earth ion radius along a, since these tetrahedra are significantly broader than the rare-earth ions. Moreover, the sodium sites residing in the relatively large voids may act as buffers yielding almost constant a values.

The structure solution of Na$_2$(Y$_{0.861(5)}$Eu$_{0.139(5)}$)(PO$_4$)(WO$_4$) proves that the trivalent europium ions occupy the rare-earth site and the refined occupation factor of Eu on this site of 13.9(5)% corresponds very well with the desired doping concentration and the respective ratio of the starting materials. Thus we were able to determine the doping concentration as well as to prove on which site the emitter is located by single-crystal X-ray diffraction. This structure is only stable up to approx. 14% Eu^{3+}. Above this concentration NaEu(WO$_4$)$_2$ and Na$_3$Eu(PO$_4$)$_2$ are formed.[18,19]
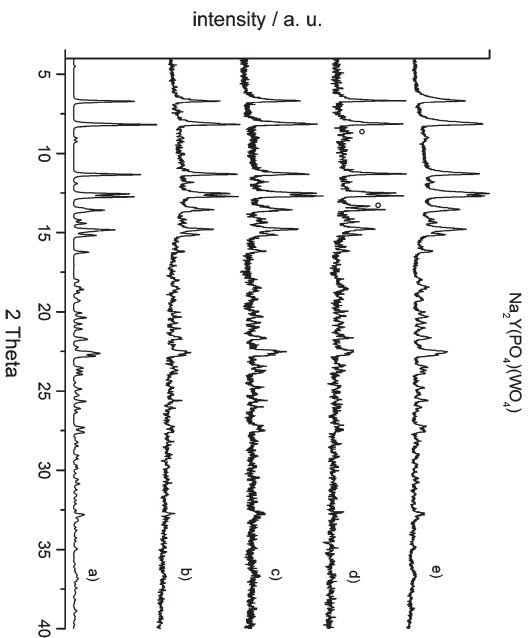
Table 1 Crystallographic data of $Na_2RE(PO_4)(WO_4)$ (RE = Y, Tb–Lu) (estimated standard deviations in parentheses)

$Na_2RE(PO_4)(WO_4)$	RE = Y	RE = $Y_{0.861(5)}Eu_{0.139(5)}$	RE = Tb	RE = Dy	RE = Ho	RE = Er	RE = Tm	RE = Yb	RE = Lu
Temperature/K					298(2)				
Crystal system					Orthorhombic				
Space group					*Ibca* (no. 73)				
a/pm	1799.7(4)	1798.65(13)	1798.8(4)	1798.9(4)	1800.8(12)	1799.2(4)	1797.9(4)	1798.8(4)	1800.8(4)
b/pm	1210.2(2)	1213.79(6)	1219.6(2)	1215.6(2)	1210.39(7)	1208.3(2)	1206.2(2)	1201.9(2)	1198.8(2)
c/pm	683.82(14)	684.57(3)	689.97(14)	687.77(14)	684.54(6)	681.48(14)	677.54(14)	676.80(14)	673.29(13)
Cell volume (10^6 pm^3)	1489.4(5)	1494.54(15)	1513.6(5)	1504.0(5)	1492.14(19)	1481.5(5)	1469.3(5)	1463.2(5)	1453.5(5)
Z					8				
Calculated density D_x/g cm^{-3}	4.261	4.415	4.807	4.869	4.930	4.986	5.043	5.101	5.153
$\mu_{MoK\alpha}$/mm^{-1}	23.528	24.477	24.789	25.480	26.272	27.108	27.987	28.759	29.667
Colour	Colourless	Colourless	Colourless	Colourless	Pink/yellow	Pink	Colourless	Colourless	Colourless
$F(000)$	1712	1775	1920	1928	1936	1944	1952.0	1960.0	1968
Radiation					Mo-K_α radiation				
Diffractometer					STOE IPDS 2				
Absorption correction					Numerical				
Index range	−21/0/0	−24/0/0	−21/0/0	−21/0/0	−24/16/9	−21/0/0	−21/0/0	−21/0/0	−20/0/0
	21/14/8	24/16/9	21/14/8	21/14/8	24/14/9	21/14/8	21/14/8	21/14/8	20/13/7
Theta range ($\Theta_{min} - \Theta_{max}$)	2.26–24.96	2.26–29.25	2.26–25.00	2.26–25.00	2.03–29.29	2.26–25.00	4.07–33.66	2.26–24.98	3.40–23.99
Reflections collected	2030	2041	2616	2599	2033	2558	2871	2510	2511
Independent reflections	661	1023	673	668	1311	658	649	648	569
Parameters	62	63	62	62	62	62	62	62	62
R_{int}	0.016	0.015	0.015	0.017	0.018	0.010	0.048	0.027	0.043
R_1(all data)	0.037	0.044	0.032	0.029	0.027	0.026	0.057	0.038	0.061
wR_2(all data)	0.040	0.054	0.036	0.038	0.037	0.042	0.077	0.066	0.124
Goodness of fit (GooF)	0.868	0.861	1.178	1.000	1.136	1.155	1.072	1.134	1.059
Residual electron density, min/max	0.63/−0.67	0.95/−1.13	1.13/−1.07	1.21/−1.48	0.74/−0.81	1.39/−1.17	1.48/−1.29	2.25/−1.70	2.48/−2.26

Table 2 Atomic coordinates and their respective isotropic and anisotropic displacement parameters/Å^2 for Na$_2$Y(PO$_4$)(WO$_4$) (estimated standard deviations in parentheses)

Atom	Wyckoff-position	x	y	z	U_{11}	U_{22}	U_{33}	U_{23}	U_{13}	U_{12}	U_{eq}/U_{iso}
Na	16f	0.59638(18)	0.1895(3)	−0.2617(6)	0.0319(15)	0.070(2)	0.0394(17)	0.001(3)	0.0019(19)	−0.0189(15)	0.0472(8)
W	8c	0.42822(2)	0	3/4	0.01569(18)	0.0228(2)	0.0283(2)	0.0016(3)	0	0	0.02225(14)
Y	8d	3/4	0.07222(7)	0	0.0190(4)	0.0102(4)	0.0111(4)	0	−0.0003(4)	0	0.0134(2)
P	8d	1/4	0.18110(18)	0	0.0209(11)	0.0114(10)	0.0115(10)	0	−0.0002(10)	0	0.0146(5)
O1	16f	0.1828(3)	0.2563(4)	0.0165(17)	0.019(2)	0.0134(18)	0.014(3)	−0.0014(17)	0.005(4)	0.003(2)	0.0154(12)
O2	16f	0.2423(3)	0.1016(3)	−0.1743(6)	0.032(3)	0.0100(19)	0.011(2)	−0.0029(17)	0.001(2)	−0.001(2)	0.0176(10)
O3	16f	0.3722(3)	−0.0251(3)	0.9580(7)	0.019(2)	0.021(3)	0.033(3)	0.0050(19)	−0.008(2)	0.0001(19)	0.0243(12)
O4	16f	0.4813(3)	−0.1158(5)	0.7073(10)	0.032(3)	0.054(4)	0.042(6)	0.003(3)	−0.001(3)	0.017(3)	0.043(2)

Table 3 Selected interatomic distances/pm and angles/° for Na$_2$Y(PO$_4$)-(WO$_4$) (estimated standard deviations in parentheses)

Y–O	225.9(4)–242.1(4)	8 distances
Na–O	228.5(7)–247.9(1)	3 distances
	276.5(8)–293.2(6)	3 distances
Y–Y	384.00(8)	
Na–Na	371.9(3), 376.5(7)	
P–O	151.8(5)–153.8(4)	
W–O	176.9(5)–172.2(6)	
O–P–O	102.5(3)–112.9(5)	
O–W–O	108.2(3)–112.5(4)	

Fig. 1 X-ray powder diffraction patterns (Mo-K$_\alpha$ radiation) of Na$_2$Y-(PO$_4$)(WO$_4$): (a) calculated from single crystal data; (b) pure phase; (c) doped with 14.5% Eu^{3+}; (d) doped with 20% Eu^{3+}; (e) doped with 12.5% Tb^{3+}.
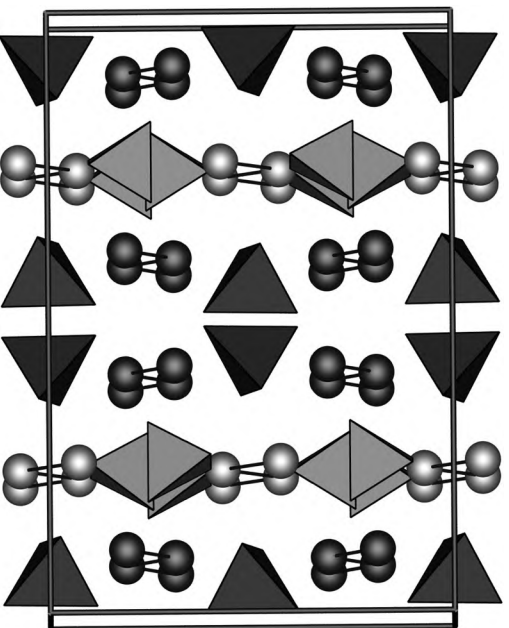
Fig. 2 Overview about the unit cell of Na$_2$Y(PO$_4$)(WO$_4$) along [001]: phosphate (gray) and tungstate (dark gray) tetrahedra are drawn as closed polyhedra, Na$^+$ as dark gray and Y^{3+} as gray spheres; the lines between the cations clarify the zigzag chains (see text) and are no bonds between the respective atoms.
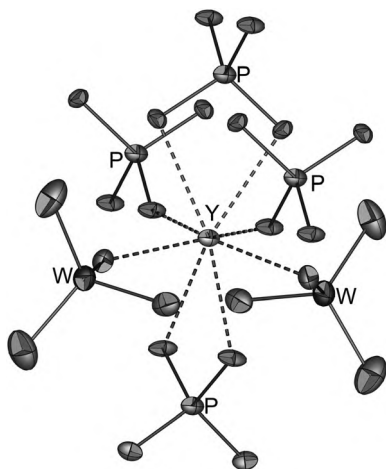
Fig. 3 Representation of the coordination environment of the yttrium atoms in $Na_2Y(PO_4)(WO_4)$, the displacement ellipsoids are drawn on a probability level of 50%.
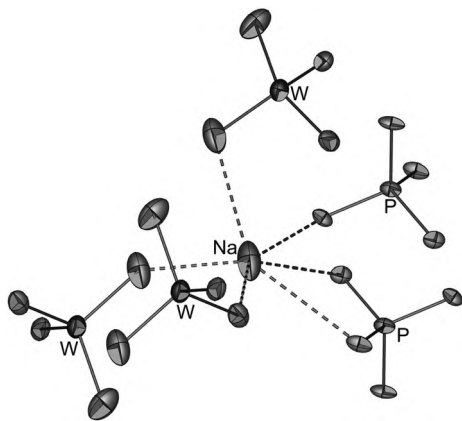
Fig. 4 Representation of the coordination environment of the sodium atoms in $Na_2Y(PO_4)(WO_4)$, the displacement ellipsoids are drawn on a probability level of 50%.

An excellent measure for deviations of tetrahedra from ideal symmetry is the method suggested by *Balic-Žunic* and *Makovicky*[13,14] which we already applied to cyclophosphates and polyphosphates like α- and β-$RE(PO_3)_3$ (RE = Sc, Y, Gd–Lu)[20] and the orthophosphate α-$BaHPO_4$,[21] where the details of this method have been also summarised. We identified typical values for condensed phosphate tetrahedra below 1%. In $Na_2RE(PO_4)$-(WO_4) (RE = Y, Tb–Lu) the deviations range from 0.50 to 0.65% for the phosphate and from 0.10 to 0.15% for the tungstate tetrahedra. Thus all values are well below this mark and all tetrahedra may be classified as regular. The smaller deviation for the tungstate tetrahedron is presumably due to the significantly higher partial charge of the central atom.

4 UV-Vis spectroscopy

The UV-Vis spectra of $Na_2RE(PO_4)(WO_4)$ (RE = Y, $Y_{0.86}Eu_{0.14}$ and Tb) are shown in Fig. 6–8. Fig. S3–S8 (ESI†) present the remaining reflection spectra. All relevant 4f–4f transitions start

from the respective ground state and are indicated according to the well known energy level schemes of the rare-earth ions.[22–24] Significant shifts of the emission lines relatively to the expected values could not be observed. In all spectra we see intense allowed W → O charge-transfer transitions which are typical for tungstates. The optical band gap of $Na_2Y(PO_4)(WO_4)$ was determined around 240 nm corresponding with 5.2(1) eV.

5 Fluorescence spectroscopy

In all the excitation spectra, the broad band in the 200–300 nm region can be assigned to the allowed W → O and Eu/Tb → O charge-transfer transitions. Fig. 9 shows the emission and excitation spectra of the orange-red phosphor $Na_2(Y_{0.86}Eu_{0.14})(PO_4)$-$(WO_4)$. We see basically the typical emissions for Eu^{3+} ions, *i.e.* the intense band from the hypersensitive transition at 615 nm ($^5D_0 \rightarrow {}^5F_2$) and the band at 592 nm ($^5D_0 \rightarrow {}^5F_1$).

In Fig. 10 the emission and excitation spectra of the green phosphors $Na_2(Y_{0.88}Tb_{0.12})(PO_4)(WO_4)$ and $Na_2Tb(PO_4)(WO_4)$ are shown. While for the pure terbium compound the maximum in the excitation spectra monitoring the emission at 544 nm is at 256 nm, it lies for the yttrium compound doped with trivalent terbium at 245 nm. The emission spectra show the typical transitions of Tb^{3+} peaking at the same wavelengths for the pure and doped compound. They are located at 489 nm ($^5D_4 \rightarrow {}^7F_6$), 544 nm ($^5D_4 \rightarrow {}^7F_5$), 584 nm ($^5D_4 \rightarrow {}^7F_4$) and 619 nm ($^5D_4 \rightarrow {}^7F_3$).

6 Band-structure calculations

For $Na_2Y(PO_4)(WO_4)$ the electronic band-structure was calculated using the full-potential linearised augmented plane wave method (FP-LAPW) embodied in the WIEN2k code[25] and the Perdew–Burke–Ernzerhof generalised gradient approximation[26,27] for the exchange and correlation correction. Atomic muffin-tin radii of 1.8 au (95.3 pm) for Na and Y, 1.7 au (89.9 pm) for W, 1.45 au (76.7 pm) for P and 1.4 au (74.1 pm) for O were used. The calculations were carried out using Monkhorst-Pack grids with 45 k points in the irreducible part of the Brillouin zone with cut-off energies $E_{pot,max}$ = 163 eV (potential) and $E_{wf,max}$ = 200 eV (interstitial plane waves). The tetrahedron method was used to integrate over the Brillouin zone to obtain total and partial densities of states (DOS, see Fig. 11). The calculated band gap of 5.1 eV corresponds well with the experimentally determined gap (5.2(1) eV). Qualitatively, the charge transfer from occupied O(p)-states to empty W(d)-states can be observed clearly in the partial DOS (pDOS, bottom part of Fig. 11). Also the states belonging to $(PO_4)^{3-}$ tetrahedra located around −2 eV are clearly separated energetically from the $(WO_4)^{2-}$ tetrahedra states around −3.3 eV.

7 Conclusions

In this contribution we elucidated the crystal structures of $Na_2RE(PO_4)(WO_4)$ (RE = Y, Tb–Lu) which are isotypic with $Na_2Y(PO_4)(MoO_4)$.[3,4] According to our experiments the larger rare-earth elements do neither form this crystal structure nor a compound of this composition but for europium at least the
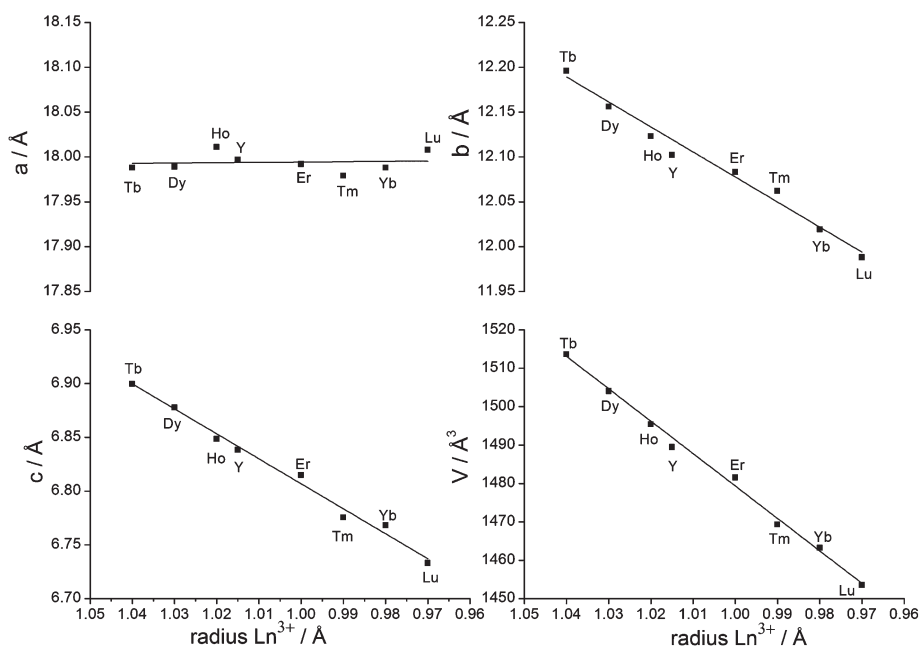
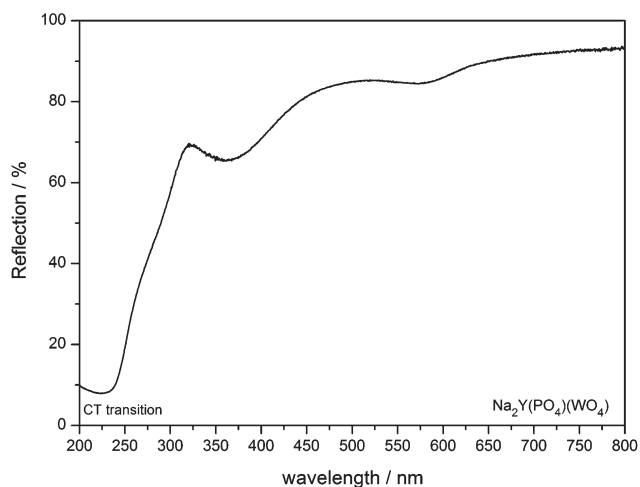**Fig. 5** Unit cell parameters plotted *vs.* the ionic radius of the rare-earth ions.
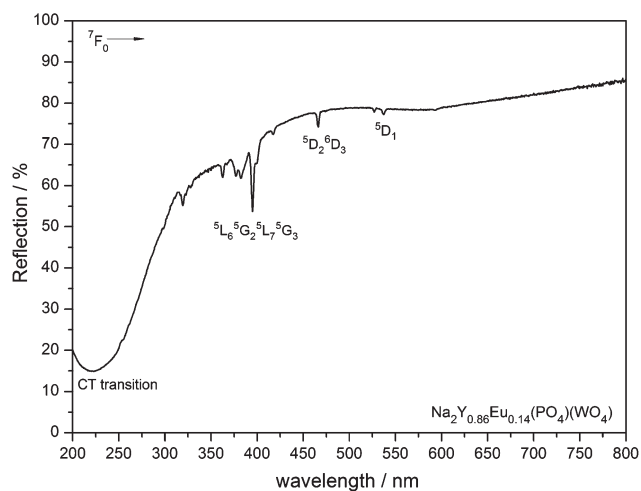

Fig. 6 UV-Vis reflection spectrum of $Na_2Y(PO_4)(WO_4)$.

Fig. 7 UV-Vis reflection spectrum of $Na_2(Y_{0.861(5)}Eu_{0.139(5)})(PO_4)$-$(WO_4)$.

highly doped representative $Na_2(Y_{0.86}Eu_{0.14})(PO_4)(WO_4)$ can be obtained. In this compound we could determine the doping concentration and prove that the europium ions only occupy the yttrium site. The estimation based on the ionic radii of Na^+, Y^{3+} and Eu^{3+} would suggest the possibility of doping europium also onto the sodium site. This can be excluded according to our single-crystal data.

$Na_2Y(PO_4)(WO_4){:}Eu^{3+}$ and $Na_2Y(PO_4)(WO_4){:}Tb^{3+}$ show the expected and typical emissions of these well known rare-earth ions. Both compounds can be excited *via* the charge-transfer transitions of tungstate. A detailed analysis of the energy-transfer mechanism will be conducted and presented in a future contribution.

A band-structure calculation confirms the presence of charge-transfer transitions within the tungstate tetrahedra as the respective states are localised around the band gap of $Na_2Y(PO_4)(WO_4)$ which was calculated to be 5.1 eV which is in fair agreement with the experimental value of 5.2(1) eV determined from the UV-Vis spectrum of $Na_2Y(PO_4)(WO_4)$.
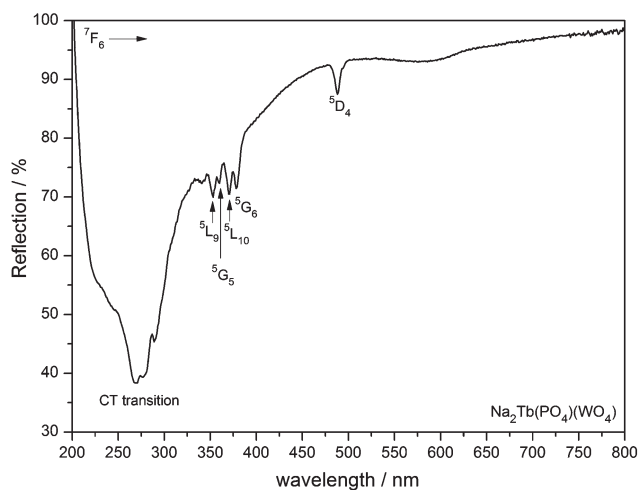
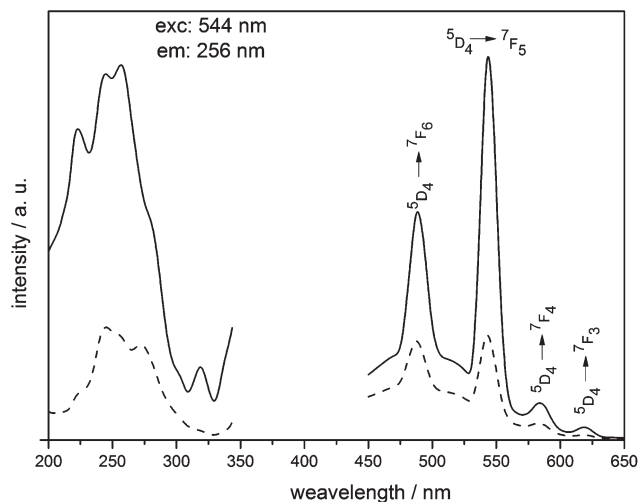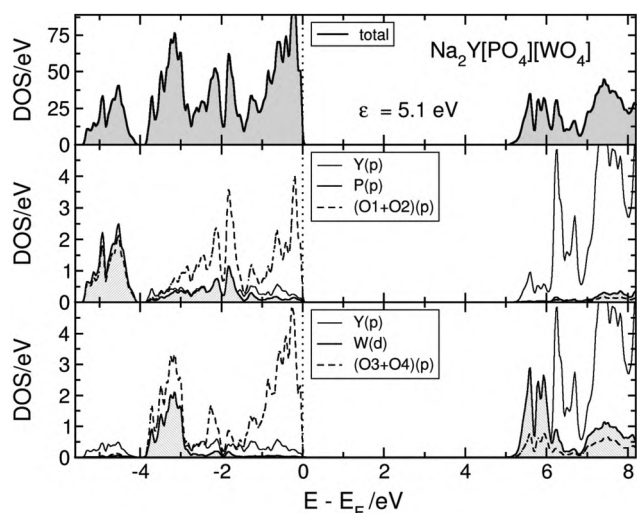**Fig. 8** UV-Vis reflection spectrum of $Na_2Tb(PO_4)(WO_4)$.
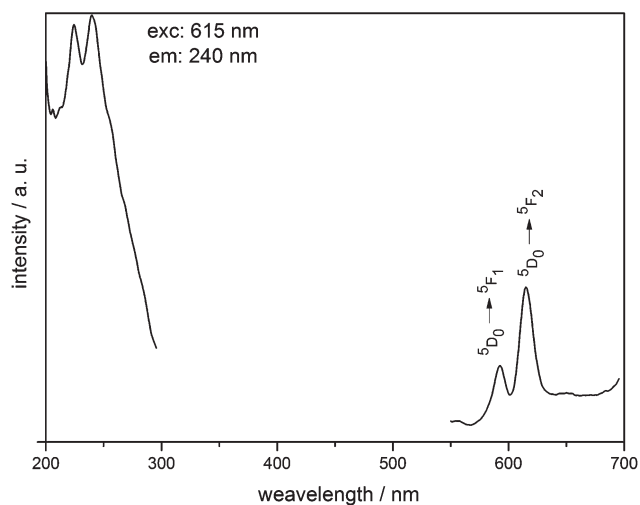
Fig. 9 Excitation and emission spectra of $Na_2(Y_{0.861(5)}Eu_{0.139(5)})(PO_4)(WO_4)$.

Fig. 10 Excitation and emission spectra of $Na_2Y_{0.88}Tb_{0.12}(PO_4)(WO_4)$ (dotted) and $Na_2Tb(PO_4)(WO_4)$ (straight line).

Fig. 11 Calculated total (top) and partial Y(p)-, P(p)- and (O1 + O2)-(p)- (middle) or Y(p)-, W(d)- and (O3 + O4)(p) (bottom) densities of states, respectively, in $Na_2Y(PO_4)(WO_4)$ (energies/eV relative to the Fermi level E_F).

References

1 S. I. Weissman, *J. Chem. Phys.*, 1942, **10**, 214–217.
2 G. Blasse and A. Bril, *J. Chem. Phys.*, 1966, **45**, 2350–2355.
3 M. Ben Amara and M. Dabbabi, *Acta Crystallogr., Sect. C: Cryst. Struct. Commun.*, 1987, **43**, 616–618.
4 R. E. Marsh, *Acta Crystallogr., Sect. C: Cryst. Struct. Commun.*, 1987, **43**, 2470.
5 M. A. Ryumin, L. N. Komissarova, D. A. Ruskaov, A. P. Bobylev, M. G. Zhizhin, A. V. Khoroshilov, K. S. Gavrichev and V. P. Danilov, *Russ. J. Inorg. Chem.*, 2007, **52**, 653–660.
6 L. N. Komissarova, M. A. Ryumin, A. P. Bobylev, M. G. Zhizhin, A. V. Khoroshilov and V. P. Danilov, *Russ. J. Inorg. Chem.*, 2006, **51**, 350–356.
7 M. A. Ryumin, V. V. Pukhkaya and L. N. Komissarova, *Russ. J. Inorg. Chem.*, 2010, **55**, 1010–1013.
8 I. V. Zatovsky, K. V. Terebilenko, N. S. Slobodyanik, V. N. Baumer and O. V. Shishkin, *Acta Crystallogr. , Sect. E: Struct. Rep. Online*, 2006, **62**, i193–i195.
9 K. V. Terebilenko, I. V. Zatovsky, V. N. Baumer, N. S. Slobodyanik and O. V. Shishkin, *Acta Crystallogr., Sect. E: Struct. Rep. Online*, 2008, **64**, i75.
10 I. V. Zatovsky, K. V. Terebilenko, N. S. Slobodyanik, V. N. Baumer and O. V. Shishkin, *J. Solid State Chem.*, 2006, **179**, 3550–3555.
11 K. V. Terebilenko, I. V. Zatovsky, V. N. Baumer and N. S. Slobodyanik, *Acta Crystallogr., Sect. E: Struct. Rep. Online*, 2009, **65**, i67.
12 D. Zhao, F. Li, W. Cheng and H. Zhang, *Acta Crystallogr., Sect. E: Struct. Rep. Online*, 2009, **65**, i78.
13 X. He, M. Guan, N. Lian, J. Sun and T. Shang, *J. Alloys Compd.*, 2010, **492**, 452–455.
14 *Programs X-Red and X-SHAPE*, Stoe & Cie, Darmstadt, 1999.
15 G. M. Sheldrick, *SHELXTL, V 5.10 Crystallographic System*, Bruker AXS Analytical X-ray Instruments Inc., Madison, 1997.
16 R. D. Shannon, *Acta Crystallogr., Sect. A: Fundam. Crystallogr.*, 1976, **32**, 751–767.
17 Y. Ni, A. M. Hughes and A. N. Mariano, *Am. Mineral.*, 1995, **80**, 21–26.
18 N. B. Manson, *Opt. Commun.*, 1982, **44**, 32–34.

19 Z. J. Chao, C. Parent, G. Leflem and P. Hagenmüller, *J. Solid State Chem.*, 1989, **82**, 255–263.

20 H. A. Höppe, *J. Solid State Chem.*, 2009, **182**, 1786–1791.

21 H. A. Höppe, M. Daub and O. Oeckler, *Solid State Sci.*, 2009, **11**, 1484–1488.

22 W. T. Carnall, P. R. Fields and K. Rajnak, *J. Chem. Phys.*, 1968, **49**, 4450–4455.

23 W. T. Carnall, P. R. Fields and K. Rajnak, *J. Chem. Phys.*, 1968, **49**, 4447–4449.

24 W. T. Carnall, P. R. Fields and K. Rajnak, *J. Chem. Phys.*, 1968, **49**, 4424–4442.

25 P. Blaha, K. Schwarz, G. K. H. Madsen, D. Kvasnicka and J. Luitz, *Wien2k – An Augmented Plane Wave and Local Orbital Program for Calculating Crystal Properties*. TU Wien, ISBN3-9501031-1-2, 2006.

26 J. P. Perdew, S. Burke and M. Ernzerhof, *Phys. Rev. Lett.*, 1996, **77**, 3865–3868.

27 J. P. Perdew, K. Burke and M. Ernzerhof, *Phys. Rev. Lett.*, 1997, **78**, 1396–1396.